



An Improved Compliant Joint Design of a Modular Robot for Descending Big Obstacles

S Phani Teja
Robotics Research Lab
IIIT Hyderabad
Gachibowli, Hyderabad, TS,
500032, India
phaniteja.sp@gmail.com

Sri Harsha
Robotics Research Lab
IIIT Hyderabad
Gachibowli, Hyderabad, TS,
500032, India
harsha.turlapati@gmail.com

Avinash Siravuru
Department of Mechanical
Engineering
Carnegie Mellon University
Pittsburgh, PA, 15213, USA
sirneonash@gmail.com

Suril V. Shah
Robotics Research Lab
IIIT Hyderabad
Gachibowli, Hyderabad, TS,
500032, India
surilshah@iiit.ac.in

K Madhava Krishna
Robotics Research Lab
IIIT Hyderabad
Gachibowli, Hyderabad, TS,
500032, India
mkrishna@iiit.ac.in

ABSTRACT

This work focuses on enhancing step descending ability of the modular robot proposed in [16]. The proposed robot consists of three modules connected with each other through passive joints. It is propelled using an active pair of wheels per module. Since there are no actuators at the joints, the joints are not susceptible to losing operability while traversing on rugged terrain. However with the absence of actuators, we face the issue of the robot toppling over when an abnormally large obstacle is encountered. This shortcoming is overcome with the use of compliant joints. The compliant joints are designed by employing springs of optimal stiffness, which is calculated through an optimization formulation aided with the constraints presented by the static analysis of the robot. The novelty lies in the systematic design of compliant joint for step descent. The robot is successful in climbing and descending obstacles of dimension 17 cm. Simulations of the mathematically modelled robot are carried out. The results from the same are validated on a working prototype and presented.

1. INTRODUCTION

The utility of robots in urban search and rescue (USAR) scenarios has been an active field of research since the last decade. One of the first deployments of robots in a real-life disaster situation has been shown post September 11 attacks on the World Trade Center [1]. Their deployment during the rescue operations after the recent earthquakes in Japan, received wide spread media attention [2, 3]. It is important that USAR robots designed for this purpose

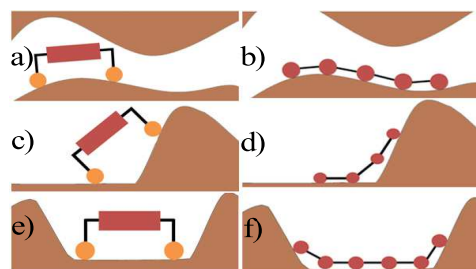


Figure 1: Different types of obstacles are shown here. A highly redundant robot (b, d and f) can perform better than a conventional mobile robot (a, c and e) in these situations

are versatile in nature to be able to handle different situations they are posed with. While navigating through the debris during a rescue mission, it may not be possible always to avoid big obstacles. Sometimes, the only way forward is to climb the obstacle. Some interesting mobile robots, such as DIR-2 [4], PAW [5], etc., were developed with enhanced climbing ability. However, their usability in USAR scenarios is limited by their size, as shown in Fig. 1 (a, c, e). Small sized and agile robots can perform better in such scenarios as is seen in nature. But, the small size puts a limit on maximum propulsive force, and thus its climbing ability. Hence, modular robots were proposed as better performers in USAR scenarios. Figure 1 illustrates the additional advantages offered by modular robots over conventional mobile robots while traversing through narrow and uneven spaces. In [6] and [7], the author described versatility, reliability and low-cost as the main advantages of such modular robots. Although versatility is given by high degrees-of-freedom, reliability by presence of multiple modules and cost effectiveness by having added traversability by simple addition/subtraction of modules, the fact that individual members have very limited mobility is a limitation. Alternatively, some researchers have also proposed to develop active/passive linking mechanisms to join multiple off-

Permission to make digital or hard copies of all or part of this work for personal or classroom use is granted without fee provided that copies are not made or distributed for profit or commercial advantage and that copies bear this notice and the full citation on the first page. Copyrights for components of this work owned by others than ACM must be honored. Abstracting with credit is permitted. To copy otherwise, or republish, to post on servers or to redistribute to lists, requires prior specific permission and/or a fee. Request permissions from permissions@acm.org.

AIR '15, July 02 - 04, 2015, Goa, India

© 2015 ACM. ISBN 978-1-4503-3356-6/15/07...\$15.00

DOI: <http://dx.doi.org/10.1145/2783449.2783518>

the-shelf or conventional mobile robots and build a train-like structures to cooperatively solve several rough terrain mobility issues, like climbing steep obstacles. Notable among them are Gunryu [8], Millibot [9] and [10]. In [16] a modular robot which can achieve mobility (by adding wheels) and compactness (by modules) was presented. While crawler robots have better climbing ability than wheeled robots, the former are slower, bulkier and have low ground clearance. It is also hard to design a water-tight and dust-proof system for crawler robots [13]. Wheels are chosen for their 1) simplicity in design, 2) speed and 3) ability to provide sufficient ground clearance. The use of active-trunk-joints for stair climbing was shown in [15] using modular robot. In [11, 13] the authors have shown that the robots with active-trunk-joints are more prone joint-motor/gear-train damage when subjected to high reaction forces/moments due to impact. On the other hand, snake-like robots with passive trunk-joints are more durable and the joints can naturally deform along the terrain. However, they can tip-over while climbing big step-like obstacles or fold inwards while descending from a particularly high ground. Hence, climbing and descending from big-step like obstacles and deep ditches, as shown in Fig. 1, is a challenging task. In [13], the authors proposed the use of strings to control the motion of the trunk, and to improve the robot's locomotion capability without any actuators at the trunk-joints. However, it still requires additional actuators for controlling the strings. Alternatively, in the present work, we extend our work of [16] and propose the use of compliant spring elements at the link-joints.

In [16], a novel AW-PJ (active-wheel passive trunk-joint) robot was proposed for climbing big step-like obstacles. It consists of modules connected by passive trunk-joints and active wheels, thus belonging to the AW-PJ category. Although the existing robot was able to traverse a variety of terrains consisting of different obstacles, there are still some problems which need to be addressed. In this paper a new problem while descending, i.e., the inward folding problem is mitigated by using an additional torsional spring at the passive trunk-joints in addition to the spring which prevents tip-over [16]. This prevents the robot from entering into unstable configurations. The design considerations and modifications to the existing compliant joint to overcome this new problem are discussed in detail.

The rest of the paper is organized as follows: Section II introduces a modular robot mechanism and discusses the step climbing and descending issues associated with passive trunk-joint robots. Section III presents an optimization formulation for designing compliant joints for successful step descent along with numerical results. Prototype construction details, experimental demonstration and numerical simulation results for unstructured terrain are shown in Sections IV and V. Finally, conclusions and future work are given in Section VI.

2. MODULAR ROBOT MODEL

The previous section discussed the robot as a member of the AW-PJ class. Our robot which was developed in [16] has active wheels which provide for propulsion. The passive trunk joints aid in the modular deformation as the robot moves through unstructured terrain. Two modules are connected by 1 degree-of-freedom (DOF) revolute joints, called trunk-joints, to achieve the required deformation over the unstructured terrain. The wheel joints and the trunk joints

are denoted by W_i and J_i respectively as shown in Fig. 2. The absolute (between module i and ground) and relative (between module i and $i + 1$) trunk joint angles are denoted by θ_i and ϕ_i , respectively, as shown in Fig. 2. Design considerations of the robot are discussed below:

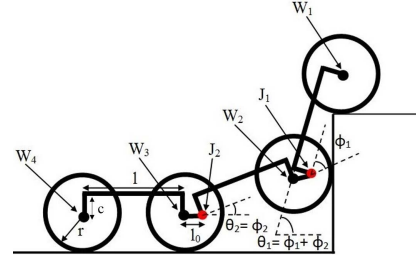


Figure 2: The front view of the robot showing the trunk and wheel joints. The relative angles (ϕ s) and absolute angles (θ s) are also depicted

2.1 Design Considerations

It worth noting that the poor design of modular robots leads to, 1) collision of trunk while climbing steps or ditches as shown in Fig. 3(a), and 2) unsuccessful climbing due to clock-wise moment generated by the normal force at the interface of wheel and step, as shown in Fig. 4(a). The above two criteria are very important in design of the proposed robot and are considered next.

2.1.1 Module Ground Clearance

Design of an appropriate ground clearance can help in avoiding any undesirable collision between the trunk and obstacles while climbing. Figure 3(b) shows the minimum clearance required, denoted as c_{min} , for avoiding collision of trunk with step. It is defined as

$$c_{min} = c + r$$

,where $c = l/2 - r\sqrt{2}$, l is length of the module and r is the wheel radius. Note that, the clearance also depends

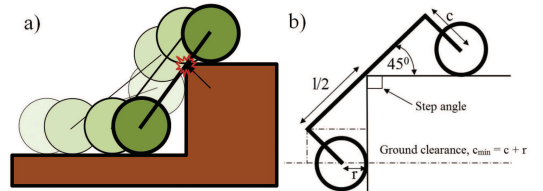


Figure 3: Effect of ground clearance: a) An inevitable collision occurs when the module is designed with insufficient ground clearance; b) The minimum ground clearance c_{min} is parametrized in terms of the length of the module(l) and the wheel radius(r).

on the shape of the obstacle, and it increases with increase in the sharpness of the obstacle/step, i.e., step angle 90° (Fig.3(b)). In this paper we focus on climbing and descending obstacle/step with step angle of 90° .

Table 1: Specifications of the 3 module robot [16]

Symbols	Quantity	Values
l	Link Length	0.15 m
b	Link Breadth	0.1 m
r	Wheel Radius	0.03 m
l_0	Wheel Joint and Link Joint Offset	0.03 m
μ	Coefficient of Friction	0.8
τ_{wmax}	Stall Torque of Wheel Motors	0.6 Nm
m_w	Mass of Each Wheel	0.1 Kg
m_l	Mass of Each Link	0.3 Kg

2.1.2 Trunk Joint Placement

Selecting the location of the trunk-joint wisely can improve the ascending and descending efficiency of the robot. Figure 4 shows two potential locations for joint placement. In Fig. 4(a), the wheel touches the step at a point lower than that of the trunk-joint. Hence, a clockwise moment will be created due to the normal force developed at the point of contact, causing the robot to fold inwards. This is undesirable, and robot will require external actuation at the trunk-joint in order to overcome the moment. This can be avoided by lowering the joint to the wheel centers, as shown in Fig. 4(b). The total moment thus created at the trunk-joint acts in the counter clockwise direction, and helps in lifting the module. This ensures natural climbing along the obstacle. The robot is wide enough to provide sufficient

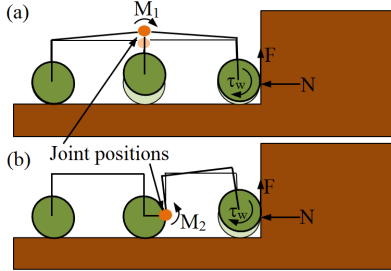


Figure 4: Two potential locations for the passive trunk-joint(PJ): a) Location 1: Clockwise moment (M_1) is created when joint is placed on the top of the module. This resists climbing ability of the robot. b) Location 2: Counter-clockwise moment (M_2) is generated when joint is positioned adjacent to the wheel axis. This naturally aids in climbing.

stability against rolling over. The specifications of the proposed robot are listed in Table I. Upon finalizing the robot's design, its step descending ability with passive trunk-joint is analysed next.

2.1.3 Descending Analysis with Passive Trunk Joint

In [16] the limiting angle called tip-over angle (θ_{to}) was defined and derived. Similarly in the case of descending a steep obstacle, we propose the fold-over condition which is defined by an inequality condition over the folding angle (θ_{f0}) as shown in Fig. 5. The condition where the passive robot tends to fold inwards while descending steep obstacles, is shown in Fig. 6. This configuration is equally undesirable. From the robot geometry, it can be noted that the limiting

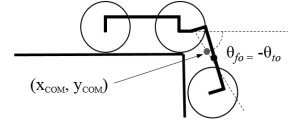


Figure 5: The folding angle of a module (θ_{f0})

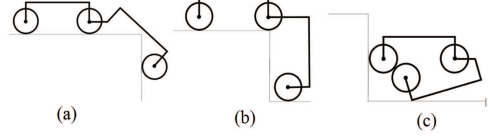


Figure 6: Snapshots of the run-up to an undesirable configuration while descending big step-like obstacle

angle during descent, defined as folding angle (θ_{f0}) is equal to $-\theta_{to}$ [16] (At this joint angle a frictional force at W_1 that contributes to a clockwise moment at the J_1 will result in the robot folding over itself as shown in Figure 6(c)). This work mainly aims to improve the descending ability of a passive modular robot proposed in [16]. In order to overcome the problem of folding, we propose the use of compliant joints consisting of torsional springs. It was shown in [16] that the use of springs during step ascent also helps in increasing the wheel traction by shifting the normal force towards climbing wheel-pairs. In this work we propose use of an additional spring which helps in solving the folding problem when the robot descends a steep obstacle. This is one of the fundamental contributions of this work. The folding configuration and the solution to this problem will be studied in sufficient detail in the next section.

3. COMPLIANT JOINT DESIGN FOR STEP ASCENT AND DESCENT

The stiffness estimation for the compliant joint is important. Making the joint too stiff prevents from achieving the desired deformation altogether which plays a pivotal role in the traversal of the robot. On the other hand, making it too loose will result in the fold-over condition taking place. Hence, it is required to obtain an optimal stiffness value of the compliant joint in question such that neither does the fold-over condition take place, nor is the deformability of the robot lost altogether. The folding configuration seen in passive robots during descent can be mitigated by having stiff resistance to clockwise moments about J_1 . Therefore, stiffness estimation is formulated as an optimization problem with the objective to minimize moments at the joints J_1 while climbing down. Note that the dynamical effects are neglected for mathematical simplicity.

3.1 Optimization Formulation and Static Model for the Compliant Robot

The calculation of the joint moments (τ), and traction and normal forces are formulated as an optimization problem. An appropriate objective function, (1) is chosen to minimize link-joint moments for the case of the descent along with the case of ascent as discussed in [16].

$$\underset{\mathbf{D}}{\text{minimize}} \quad \sum_{j=1}^p \tau^j \quad (1)$$

where, $\boldsymbol{\tau} = [\tau_1 \ \tau_2]^T$, $\mathbf{F} = [F_1 \ F_2 \ F_3 \ F_4]^T$, $\mathbf{N} = [N_1 \ N_2 \ N_3 \ N_4]^T$, and the vector of design variable $\mathbf{D} = [\mathbf{F}^T \ \mathbf{N}^T \ \boldsymbol{\tau}^T]^T$. Moreover, F_i 's and N_i 's denote traction and normal forces acting at wheel-pair i , and τ_i 's denote the moments at the link joints. Eq. (1) is subjected to friction ($F \leq \mu$) and static stability constraints.

A planar quasi-static analysis of this modular robot can approximate its real behaviour as it is symmetric about the sagittal plane. A generalized set of equations for any arbitrary configuration can be obtained as long as the wheels stay in contact with the ground, which is the case in CRAB [17] and PAW [5]. However, here, the static stability equations change when wheel-pair leaves contact with the ground during ascent as well as descent. Hence, different set of equations have to be considered for different configurations of the robot while optimization. Different configurations attained and the equations for each phase, of the robot ascending a step can be found in our previous work [16]. The configurations attained during descending steep obstacles are shown in Fig 7.

The analysis for descent is split into two phases. In the first phase only the first link is descending, as shown in Fig. 7(a) and in the second phase, both the first and second links descend, as shown in Fig. 7(b). In phase-1, the robot descends a height of upto $l \sin \theta_f$ while in phase-2, it descends heights between $l \sin \theta_f$ to $2l \sin \theta_f$. The static stability equations undergo minor changes to reflect the change in robot geometry. Equations for Phase-1 and Phase-2 of descending steep obstacles are given below in (2) and (3), respectively.

One module descending

$$\begin{aligned} \sum F_x &= 0 & N_1 + F_2 + F_3 + F_4 &= 0 \\ \sum F_y &= 0 & 3w_l + 8w_w + 2F_1 - 2N_2 - 2N_3 - 2N_4 &= 0 \\ \sum M_{J_1} &= 0 & 2F_1(l \cos \phi_1 - r) - 2N_1 l \sin \phi_1 + 2w_w l \cos \phi_1 \\ & & + w_l[(l/2) \cos \phi_1 + c \sin \phi_1] - \tau_1 &= 0 \\ \sum M_{J_2} &= 0 & 2F_2 r + 2N_2 l - 2w_w l - w_l(l/2) - \\ & & [(2w_w + w_l) + 2F_1](l + l_0) - \tau_1 + \tau_2 &= 0 \end{aligned} \quad (2)$$

Two modules descending

$$\begin{aligned} \sum F_x &= 0 & N_2 + F_3 + F_4 &= 0 \\ \sum F_y &= 0 & 3w_l + 8w_w + 2F_2 - 2N_3 - 2N_4 &= 0 \\ \sum M_{J_1} &= 0 & 2w_w l \cos(\phi_1 + \phi_2) + w_l[(l/2) \cos(\phi_1 + \phi_2) + \\ & & c \sin(\phi_1 + \phi_2)] - \tau_1 &= 0 \\ \sum M_{J_2} &= 0 & 2w_w(l) \cos \phi_2 + w_l[(l/2) \cos \phi_2 + c \sin \phi_2] + \\ & & [(2w_w + w_l)(l + l_0) \cos \phi_2 + 2F_2(l \cos \phi_2 - r) \\ & & - 2N_2 l \sin \phi_2 + \tau_1 - \tau_2] &= 0 \\ \sum M_{W_4} &= 0 & 2F_3 r + 2F_4 r + 2N_3 l - 2w_w l - w_l(l/2) \\ & & - [2(2w_w + w_l + F_2)](l + l_0) + \tau_2 &= 0 \end{aligned} \quad (3)$$

where τ_{wi} is the i th wheel torque, w_l ($m_l g$) and w_w ($m_w g$) are the weights of the link and wheel-pair respectively. For

Phase-1, $\phi_1 = \theta_1 = \sin^{-1}(h/l)$ and $\phi_2 = 0$, and for Phase-2, $\phi_2 = \theta_2 = \sin^{-1}(h - l \sin \theta_{to})/l$ and $\phi_1 = \theta_{to} - \phi_2$. Here, the second module will begin to climb down only after the first module reaches $l \sin \theta_{to}$. In Phase-2, ϕ_1 is designed such that if ϕ_2 increases ϕ_1 decreases by the same amount maintaining $\theta_1 = \theta_{to}$, in order to avoid tipping over.

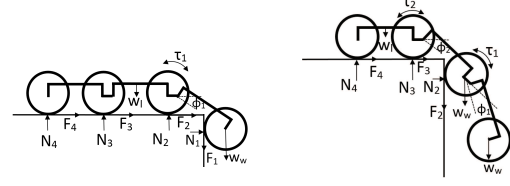


Figure 7: The forces and moments are shown for the two possible descent configurations ie., a) Phase-1: when only one module is descending and b) Phase-2: when two modules are descending

Generally, torsional springs are unidirectional in nature. Therefore the spring that can resist counter clockwise moments at J_1 during positive angular displacements, cannot apply resisting clockwise moments when there is a negative angular displacement. Therefore, two springs will be used instead. Accordingly, the static analysis is also decoupled. Note that, τ_1 and τ_2 will always act in such a way that they balance the net moments at J_1 and J_2 , respectively. The torsional springs that resist tip-over while climbing up are compressible springs which only act when there is a positive displacement of angle ϕ_1 . Therefore, an additional spring needs to be added to the robot such that it only acts for negative displacements of ϕ_1 , thus avoiding the undesirable folding configuration occurring during descent.

3.2 Joint Stiffness Estimation

After performing optimization, the obtained profiles of joint moments (τ) versus joint angles ($\phi = [\phi_1 \ \phi_2]^T$) were plotted and are shown in Fig. 8 with a solid curve for the joint J_1 . Since the profiles are nearly linear, least squares

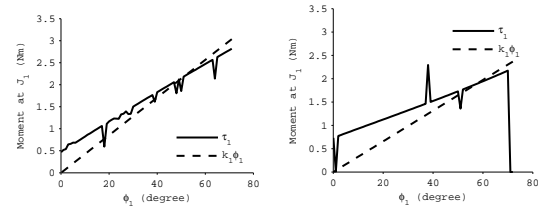


Figure 8: Moment plots for joint J_1 : The plots shows the desired moments obtained from the optimization procedure (solid line) and the moments generated by the optimal spring (dotted line) for Step Ascent and Descent, respectively. The slope of the the dotted line yields the spring stiffness value

approximation is carried out to obtain the optimum stiffness values for the joint J_1 for the case of ascent and descent. In the case of joint J_2 , the obtained profile for the case ascent had been shown in [16]. In the case of descent, the action of spring at J_2 in the negative (clockwise) direction results in the loss of contact of W_4 leading to an unstable configuration of the robot, hence, no spring is used in the negative

direction.

The values of stiffness for J_1 , k_1 , were determined as $0.0427 \text{ N} - \text{m/deg}$ for ascent and $0.0329 \text{ N} - \text{m/deg}$ for descent. The stiffness value for J_2 , k_2 , is of order 10^{-6} for the case of ascent and hence, it is assumed to be zero. According to the results obtained from the above optimization procedure, compliant joints were developed for the joints.

4. NUMERICAL RESULTS FOR STEP ASCENT AND DESCENT

The step ascending ability of the modular robot was tested for different cases [16] and it was shown that using a compliant joint at J_1 increased the normal reaction N_1 , and hence F_1 which facilitated the wheel-1 to climb up the riser without slipping. It was also shown that the slip-rate was found to be more bounded by the use of the compliant joints. It was also shown that using a spring at J_2 having the same stiffness value as J_1 enhanced the climbing ability of the robot.

This work mainly focuses on the step descending ability of the modular robot. Numerical simulations were conducted for different heights of the step to show the efficacy of the robot. Fig. 9 (a)-(c) shows the folding of the robot in absence of the second spring at J_1 in the case of 14 cm height obstacle. Subsequently, after adding the second spring at J_1 , the robot successfully descended the step as shown in Fig. 9 (d)-(f). Even during step descent, it was observed that having compliance only at joint J_1 avoided folding for heights lower than $l \sin \theta_f$. While descending from bigger heights, the same phenomenon is noticed at J_2 . This can be avoided by the introduction of a counter clockwise spring at J_2 having the same stiffness value as J_1 . Though ascent is more energy consuming, it is easier to control. On the other hand, descent is much harder to control passively, as the modules are being pulled down by gravity. During step ascent, springs help to avoid tip over and redistribute normal force among climbing members. However, they play a different role during descent. Here, they resist the links from

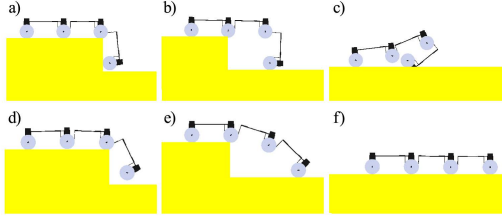


Figure 9: Step descending ability of the robot: a)-c) Case-1: The robot folds on to itself while descending a step of 14 cm; d)-f) Case-2: it successfully descends a step of 14 cm height with the introduction of another spring (for clockwise moment) at J_1

grazing the step's riser while descending. This configuration, as shown in Fig. 6(b), typically leads to the undesirable folding configuration. The wheels are made to lose contact with the step, as shown in Fig. 9(d) by the addition of another spring at J_1 . This way, when they land on the ground, the weight moments naturally straighten the module, as shown in Fig. 9(e)-(f). It can be noted that the springs used for avoiding tip-over cushion the fall during descent. Further ex-

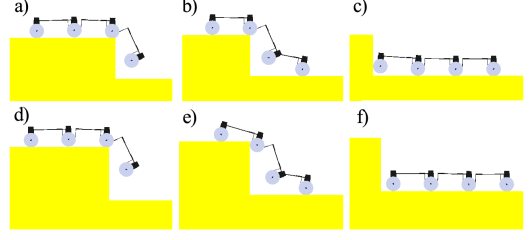


Figure 10: Case a)-c): The robot descending a step of 17 cm height; Case d)-f): The robot descending a step of 22 cm height.

periments were conducted for testing the robustness of the robot during the descent and it was found that the robot can climb down a step of height as high as 22 cm without folding onto itself with introduction of a spring at J_2 as discussed. Fig 10. shows the simulation results of the robot descending a steps of height 17 cm, Fig. 10(a-c) and 22 cm, Fig. 10(d-f).

In this section, it was shown that a modular robot having compliant joints at J_1 and J_2 can successfully climb and descend from obstacles that are upto 3 times its wheel diameter and a little greater than its body length. It was also shown that the robot can descend heights more than 3 times its wheel diameter and the it is much robust in the descent case when compared to the case of ascending. The robot can climb much higher (upto 30 cm) without tipping over, but it lacks propulsive force to pull the remaining modules to the top. Adding more modules does enable it to climb greater heights. This was shown in [16]. In that work, it was also shown how this design methodology can be extended to an n-modular robot, to determine the maximum height that it can climb and the number of compliant joints required for the same.

5. EXPERIMENTAL DEMONSTRATION

In the previous section, extensive numerical and simulation studies were carried out to demonstrate the importance of compliant joints in improving the climbing and descending ability of the robot. In order to validate these numerical results, experimental prototype of a compliant robot with 2 springs at J_1 was developed. Its climbing and descending abilities were assessed on different types of obstacles, first numerically, and then experimentally. Various experiments showing the climbing ability of the robot were presented in our previous work [16]. In this work the descending ability of the robot has been tested for different heights. The prototype is shown descending a step of 17 cm height in the Fig. 11 and a step of 22 cm in Fig. 12 which are some of the extreme cases the robot can descend. In addition to

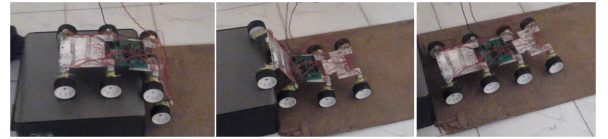


Figure 11: Robot climbing down 17cm height step
structured obstacles, the robot's traversing ability was also

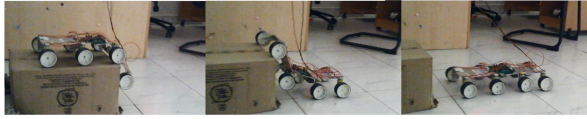


Figure 12: Robot climbing down 22cm height step

numerically tested and successfully verified on an unstructured terrain, as shown in Fig. 13. One of the key advantages of modular robots is compact design, low height and high articulation. This makes them ideally suited to traverse through tight spaces, clearly demonstrating the robustness of the robot.

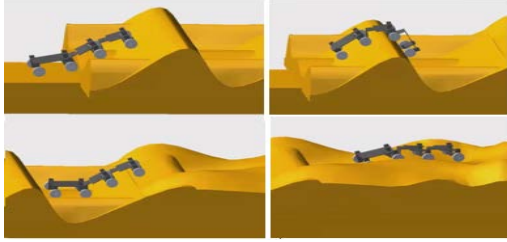


Figure 13: The 3-module compliant robot traversing on a highly uneven terrain

6. CONCLUSIONS

In [16], we proposed a modular compliant robot that can ascend big, steep step-like obstacles and traverse on a highly uneven terrain. In this work we have extended the capability of this robot to successfully descend steep obstacles by proposing an additional spring at the first compliant joint of the robot. We obtained the stiffness values for the compliant joints by posing it as an optimization problem over the quasi-static model of the modular robot as it traverses through the said terrain. Backed with this theoretical understanding of the proposed robot, a 3-module compliant robot was successfully simulated for descending heights upto 22 cm. The additional spring was fabricated and added to the experimental prototype of the 3-module robot [16] to validate the results of simulation. It is shown that the compliant joints helps in avoiding fold-over condition of the robot. The experimental results of steep obstacle descending were also shown.

Currently, the robot's motion is planar along the sagittal plane. The major focus of the future work is develop compliant yaw and roll joints also, to enable traversing on a full 3D unstructured environment. Secondly, spring stiffness values are sometimes task specific. Therefore, the possibility of using parallel elastic actuators to dynamically control the spring stiffness for different rough terrain maneuvers will also be explored.

7. REFERENCES

- [1] A. Davids, Urban search and rescue robots: from tragedy to technology, *IEEE Intelligent Systems*, 2002.
- [2] Erico Guizzo, Japan earthquake: Robots help search for survivors, *IEEE Spectrum*, 2011.
- [3] Erico Guizzo, Japan earthquake: More robots to the rescue, *IEEE Spectrum*, 2011.
- [4] A. Kamimura and H. Kurokawa, High-step climbing by a crawler robot dir-2-realization of automatic climbing motion, In *IEEE/RSJ International Conference on Intelligent Robots and Systems (IROS)*, 2009.
- [5] K. Turker, I. Sharf, and M. Trentini, Step negotiation with wheel traction: a strategy for a wheel-legged robot, In *IEEE International Conference on Robotics and Automation (ICRA)*, 2012.
- [6] Mark Yim, David G Duff, and Kimon Roufas, Modular reconfigurable robots, an approach to urban search and rescue, *1st International Workshop on Human-friendly Welfare Robotics Systems*, 2000.
- [7] Mark Yim, Wei-Min Shen, Behnam Salemi, Daniela Rus, Mark Moll, Hod Lipson, Eric Klavins, and Gregory S Chirikjian, Modular self-reconfigurable robot systems [grand challenges of robotics], *IEEE Robotics & Automation Magazine*, 2007.
- [8] Shigeo Hirose, Takaya Shirasu, and Edwardo F Fukushima, Proposal for cooperative robot gunryu composed of autonomous segments, *Robotics and Autonomous Systems*, 1996.
- [9] H. Benjamin Brown, J.M. Vande Weghe, C.A. Bererton, and P.K. Khosla, Millibot trains for enhanced mobility, *Mechatronics, IEEE/ASME Transactions on*, 2002.
- [10] Ashish Deshpande and Jonathan Luntz, Behaviors for physical cooperation between robots for mobility improvement, *Autonomous Robots*, 2007.
- [11] Hitoshi Kimura and Shigeo Hirose, Development of genbu: Active wheel passive joint articulated mobile robot. In *IEEE/RSJ International Conference on Intelligent Robots and Systems (IROS)*, 2002.
- [12] Tetsushi Kamegawa, Tatsuhiro Yamasaki, Hiroki Igarashi, and Fumitoshi Matsuno, Development of the snakelike rescue robot, In *IEEE International Conference on Robotics and Automation (ICRA)*, 2004.
- [13] Kousuke Suzuki, Atsushi Nakano, Gen Endo, and Shigeo Hirose, Development of multi-wheeled snake-like rescue robots with active elastic trunk, In *IEEE/RSJ International Conference on Intelligent Robots and Systems (IROS)*, 2012.
- [14] Mark Yim, Sam Homans, and Kimon Roufas, Climbing with snake-like robots, In *IFAC Workshop on Mobile Robot Technology*, 2001.
- [15] Arun Kumar Singh, Rahul Kumar Namdev, Vijay Eathakota, and K Madhava Krishna, A novel compliant rover for rough terrain mobility, In *IEEE/RSJ International Conference on Intelligent Robots and Systems (IROS)*, 2010.
- [16] Siravuru Avinash, Ankur Srivastava, Akshaya Purohit, Suril V Shah, and K Madhava Krishna, A compliant multi-module robot for climbing big step like obstacles, In *IEEE International Conference on Robotics and Automation (ICRA)*, Hong Kong, China, 2014.
- [17] Ambroise Krebs, Thomas Thueer, Stephane Michaud, and Roland Siegwart, Performance optimization of all-terrain robots: a 2d quasi-static tool, In *IEEE/RSJ International Conference on Intelligent Robots and Systems (IROS)*, 2006.